Substituted dipyridophenazine complexes of Cr(III): Synthesis, enantiomeric resolution and binding interactions with calf thymus DNA

Substituted dipyridophenazine complexes of Cr(III): Synthesis, enantiomeric resolution and binding interactions with calf thymus DNA†

Suni Vasudevan,[a] Jayden A. Smith,[a] Michal Wojdyla,[a] Thomas McCabe,[a] Nicholas C. Fletcher,[b] Susan J. Quinn‡[a] and John M. Kelly*[a]

Received 6th January 2010, Accepted 19th February 2010
First published as an Advance Article on the web 18th March 2010
DOI: 10.1039/c000150c

$[Cr(phen)_2(X_2dppz)]^{3+}$ {X = H, Me, or F} have been synthesised, characterised, and chromatographically resolved into their constituent Δ and Λ enantiomers. The DNA-binding interactions of each of the racemic complexes were investigated, with the results of linear dichroism, thermal denaturation, and emission quenching studies indicative of intercalative binding to CT-DNA with a significant electrostatic contribution. UV/Vis absorption titrations suggest strong DNA binding by each of the racemic complexes, with the methylated analogue $[Cr(phen)_2(Me_2dppz)]^{3+}$ exhibiting the largest equilibrium binding constant. Emission quenching and UV-Vis titrations of the enantiomers of $[Cr(phen)_2(dppz)]^{3+}$ imply similar binding affinities for the Δ and Λ isomers, although significant differences between the circular dichroism spectra of the enantiomers in the presence of DNA connote differences in binding orientation and/or conformation between the two.

1. Introduction

The design of drugs to direct photooxidative damage to specific sites on nucleic acids opens up the possibility of inhibiting transcription and DNA replication in tumour cells.[1] One group of complexes, which are known to bind to DNA and whose spectroscopic and electrochemical properties can be tuned, are metal polypyridyl complexes.[2] Transition metal complexes of dipyridophenazine (dppz) and its derivatives have been of particular interest for many years, partly because of the properties of $[Ru(bpy)_2(dppz)]^{2+}$ which is non-luminescent in water but luminesces when it intercalates into DNA.[3] Contrasting behaviour is found for $[Ru(TAP)_2(dppz)]^{2+}$ which is luminescent in water but not when bound to DNA.[4] This latter phenomenon has been ascribed to the reduction of the excited state of the complex by guanine; the process probably proceeding by proton coupled electron transfer (PCET).[4]

The DNA-binding of dppz complexes of other transition metals, such as platinum,[5] iridium,[6] rhodium,[7] rhenium[8] and chromium[9] have also been investigated. The chromium(III) complexes are particularly interesting as the photophysics of such species is expected to be determined by metal-centred (MC) states in contrast to the metal-to-ligand charge transfer (MLCT) states of their ruthenium(II) analogues. They are also expected to be better photoxidising agents and indeed Kane-Maguire and co-workers have previously shown that when $[Cr(phen)_2(dppz)]^{3+}$ binds to DNA the ^2E emission is quenched, presumably a consequence of photo-induced electron transfer.[10]

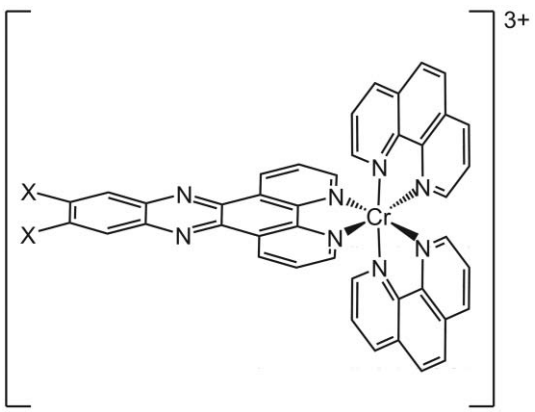

X = H, Me, or F

In order to study this type of complex more thoroughly, and to determine the effect of substitution in the dppz-ligand, we have synthesised the three complexes **1-3**, resolved the Δ and Λ enantiomers, and studied their binding to mixed sequence DNA using UV/Vis absorption and emission spectroscopy, complemented by both circular and linear dichroism studies.

2. Results and discussion

2.1. Synthesis and characterisation

The ligands dppz, Me_2dppz and F_2dppz were synthesised by reported methods.[11,12] The complexes **1–3** were prepared by refluxing the appropriate X_2dppz ligand overnight with a precursor complex $[Cr(phen)_2(CF_3SO_3)_2]CF_3SO_3$, itself produced

[a]*School of Chemistry and Centre for Chemical Synthesis and Chemical Biology, University of Dublin, Trinity College, College Green, Dublin 2, Republic of Ireland. E-mail: jmkelly@tcd.ie; Fax: +353 1 671 2826*
[b]*School of Chemistry and Chemical Engineering, Queens University Belfast, Stranmillis Road, Belfast, BT9 5AG*

† Electronic supplementary information (ESI) available: UV/vis absorption titrations, steady state emissions, and CD titrations of complexes with CT-DNA; selected bond lengths and bond angles of crystals of **1** and **3**; packing diagrams of crystals **1** and **3**. CCDC reference numbers 761094 and 68103. For ESI and crystallographic data in CIF or other electronic format see DOI: 10.1039/c000150c

‡ Present address: School of Chemistry and Chemical Biology and Centre for Chemical Synthesis and Chemical Biology University College Dublin, Belfield, Dublin 4, Republic of Ireland.

from the dichloro complex $[Cr(phen)_2Cl_2]Cl$ (Scheme 1). It is worth mentioning that the synthesis of the precursor complex $[Cr(phen)_2(CF_3SO_3)_2]CF_3SO_3$ was attempted several times in our lab adapting reported procedures,[9a,13] however with varying success. After repeated trials and carefully evaluating the conditions, a modified procedure was developed with improved yield and reproducibility, as described in the experimental section. Complexes were further purified by cation-exchange chromatography and isolated as their PF_6 salts. Spectral and structural characterisation of the complexes were concordant with the expected values (NMR spectra could not be obtained due to the paramagnetic nature of the Cr(III) centre.) Although the complexes were found to be stable as solids at room temperature, all were found to slowly decompose in aqueous solution and to undergo photosubstitution under strong UV radiation.

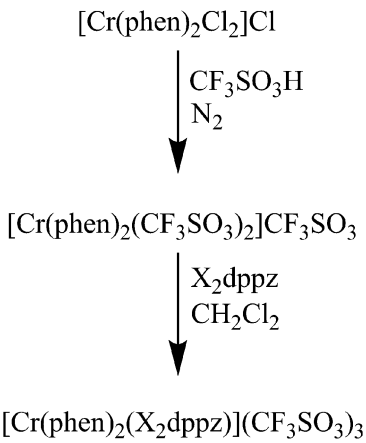

Scheme 1 Synthetic route to the preparation of $[Cr(phen)_2(X_2dppz)](CF_3SO_3)_3$.

The electronic spectra of the complexes (Fig. 1) reveal ligand-centred absorptions around 270–280 nm, dipyrido-phenazine $\pi\rightarrow\pi^*$ transitions in the 350–390 nm region and a low intensity shoulder at about 420 nm which is possibly due to d-d transitions.

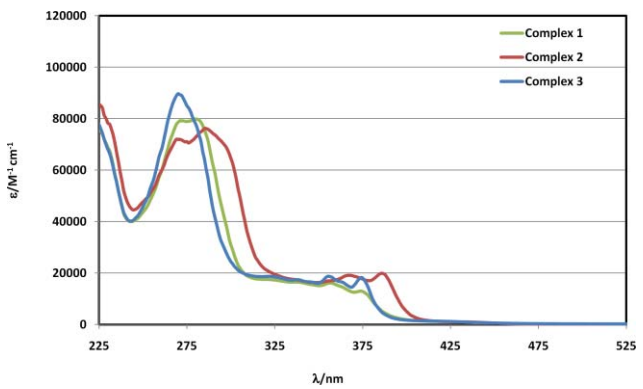

Fig. 1 Electronic absorption spectra of the complexes $[Cr(phen)_2(X_2dppz)](PF_6)_3$ {X = H, Me, or F} in acetonitrile.

The redox properties of the complexes were investigated by cyclic voltammetry. Complexes **1-3** revealed a reversible Cr(III)/Cr(II) couple in 0.1 M KCl electrolyte and $E°(Cr^{3+}/Cr^{2+})$ (*vs* NHE) were determined as -0.18 V (for **1**), (-0.17 V in ref. 13), -0.22 V (for **2**), and -0.089 V (for **3**), consistent with the electron donating/withdrawing nature of the substituent groups.[14]

The two enantiomers of complex **1** were successfully resolved using cation-exchange chromatography on Sephadex C-25 with an eluent containing the chiral anion {(–)-*O*,*O*′-dibenzoyl-L-tartrate}. Enantiomeric purity was assayed by CD spectroscopy (Fig. 2), with the absolute configurations of the enantiomers assigned by comparison with similar complexes of known configuration.[15,16] In each instance the Λ enantiomer was found to elute before the Δ enantiomer.

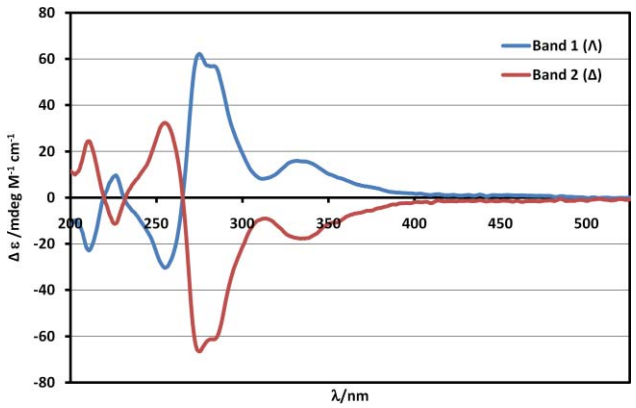

Fig. 2 CD spectra of the enantiomers of $[Cr(phen)_2(dppz)](PF_6)_3$ in acetonitrile.

2.2. Crystal structure of *rac*-$[Cr(phen)_2(dppz)](CF_3SO_3)_3$ (1) and *rac*-$[Cr(phen)_2(F_2dppz)](CF_3SO_3)_3$ (3)

Crystal structures for both the dppz and F_2dppz complexes were obtained. Single crystals suitable for X-ray diffraction of *rac*-**1** were isolated by slow evaporation of a methanolic solution, while crystals of *rac*-**3** were grown from an acetonitrile–water mixture solution. Fig. 3 and 4 reveal the molecular structures of the compounds **1** and **3** with the atom numbering scheme. The crystal data and structural refinement parameters are given in Table S1. In both the complexes, the central chromium atom exists in a six-coordinated environment connected to six nitrogen atoms from two phenanthroline and one dipyridophenazine ligand.

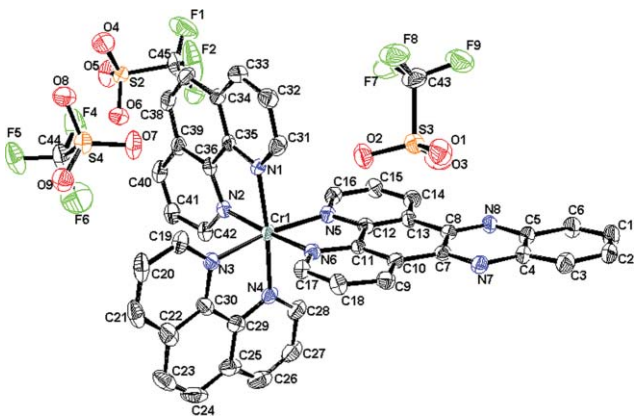

Fig. 3 Molecular structure of *rac*-$[Cr(phen)_2(dppz)](CF_3SO_3)_3$ (*rac*-**1**) with the atomic numbering scheme. Ellipsoids are shown with 50% probability. For clarity hydrogen atoms are not shown.

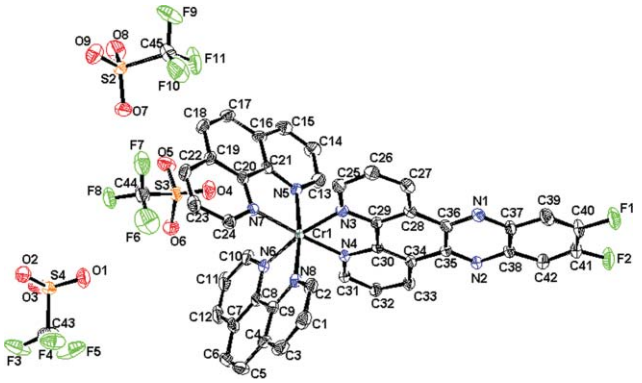

Fig. 4 Molecular structure of *rac*-**3** $[Cr(phen)_2(F_2dppz)](CF_3SO_3)_3$ with the atomic numbering scheme. Ellipsoids are shown with 50% probability.

A distorted octahedral (O_h) geometry is suggested for the complex **1** with similar Cr–N bond-lengths in the square plane (*ca.* 2.05 Å), and slightly different equatorial bonds (Cr1–N3 2.062(4) Å; Cr1–N5 2.049(4) Å). The bite angles N1–Cr1–N2 (80.69(16)°); N3–Cr1–N4 (81.14(17)°) and N5–Cr1–N6 (80.26(16)°) also support the distorted O_h geometry. The bonding and structure of the difluoro-complex **3** is similar to that of **1** with almost identical bond lengths and angles (Table S2†). The dppz and F_2dppz moieties are almost planar establishing the possibility for intercalation into DNA base pairs. The fluorine atoms F1 and F2 do deviate somewhat from the mean plane of the dppz moiety potentially influencing the intercalation of the complex between DNA base pairs.

The X-ray diffraction data reveal the presence of the two enantiomers in the unit cell, which form the basic unit of the crystal packing (Figs. S2 and S3†). The enantiomers repeat as one-dimensional columns along the 'a' axis, and two neighbouring one-dimensional arrays are then linked by the triflate anions. This creates a three-dimensional zig-zag packing in the crystal lattice. Some additional C–H—π and H bonding interactions stabilise the packing.

2.3. DNA binding interactions

2.3.1. UV/vis absorption studies. The addition of calf thymus DNA (CT-DNA) to the chromium(III) dipyridophenazine complexes causes significant changes in their absorption spectra. As an example, the absorption spectra for *rac*-$[Cr(phen)_2(F_2dppz)](CF_3SO_3)_3$ (*rac*-**3**) in the presence of increasing concentration of CT-DNA is presented in Fig. 5. The changes in the spectrum indicate that the complex possesses a strong affinity for CT-DNA. A distinctive effect of the binding to DNA is a significant hypochromism of the dppz π→π* bands (in the case of *rac*-**3**, for example, this is found to be 52% at 377 nm). This decrease in intensity is also accompanied by a slight redshift (about 2 nm) of both bands. At higher DNA concentration the relative absorption intensities of π→π* transitions tend to saturate (see ESI Fig. S4†). Concurrently the intensity of shoulders at longer wavelengths increase with DNA concentration leading to the appearance of characteristic isobestic points at 386 nm (*rac*-**1**), 398 nm (*rac*-**2**), and 384 nm (*rac*-**3**) respectively (see Fig. S5 and S6†).

The equilibrium constants were determined from the Scatchard plots calculated using the unbound and bound complex concentrations at the various DNA concentrations. The inset of Fig. 5 shows the Scatchard plot for *rac*-$[Cr(phen)_2(F_2dppz)](CF_3SO_3)_3$. The binding isotherms were fitted using the excluded site model of McGhee and von Hippel. Analysis yielded association equilibrium constants (K_{DNA}) and site exclusion parameters (n base-pairs) values of 3.1×10^5 ($n = 3.5$), 1.5×10^6 ($n = 2.7$), 1.8×10^5 M^{-1} ($n = 2.7$) for *rac*-**1**, *rac*-**2** and *rac*-**3** respectively. The results for *rac*-**1**, where binding causes a redshift of 2 nm and a 33% hypochromism at 377 nm, are in excellent agreement with similar determinations done previously by Barker *et al.*[16] The highest binding constant is exhibited by *rac*-**2**, which is consistent with the hydrophobic nature of the methyl substituents and the expected entropic benefit of secreting these groups deep within the DNA helix.[17,18] This complex also exhibited the largest red shift of the dppz π→π* bands (~ 5 nm) with a 46% hypochromism at 389 nm.

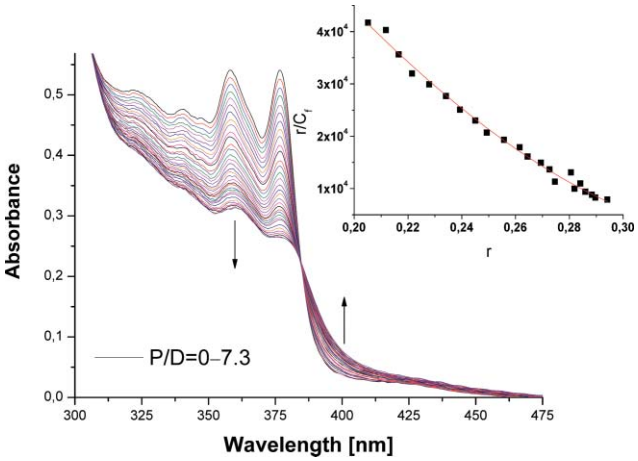

Fig. 5 UV/vis absorption spectra of *rac*-$[Cr(phen)_2(F_2dppz)](CF_3SO_3)_3$ (*rac*-**3**), (24 μM in 100 mM phosphate buffer solution, pH=7.4) in the presence of increasing concentrations of CT-DNA (P:D = nucleotide:Cr = 0–7.3). Inset: The Scatchard plot for *rac*-**3** calculated using the absorbance at 377 nm (r is the average number of bound complexes per base pair, C_f is the concentration of the unbound complexes). The data were fitted between 20% and 90% bound complexes using the McGhee and von Hippel model. Nonlinear least squares regressions were done in 'Origin 7.5' based on the Levenberg-Marquardt algorithm.

The binding of the Δ- and Λ- enantiomers of $[Cr(phen)_2(dppz)]Cl_3$ with CT-DNA were also examined using UV/vis aborption spectroscopy. (Fig. S7†). Both the enantiomers were found to bind strongly to DNA, with spectroscopic changes similar to those observed for the racemic complex.

2.3.2. Emission quenching studies. All three complexes in aqueous solution exhibit strong, room temperature emission even when the solution is air-saturated. Normalised emission spectra were found to be almost identical for all three complexes (Fig. 6; ESI Fig. S8†). This metal-centred phosphorescence which results from transitions between probably thermally equilibrated ^2E_g and $^2T_{1g}$ states to the $^4A_{2g}$ (O_h) ground state shows maximum intensity at 730 nm (Fig. 6). In accord with this, changing the substituent on the dppz-ligand has little influence on the energy levels of the lowest emitting states. In the presence of increasing concentrations of CT-DNA, very strong quenching of the phosphorescence signal is observed for all three complexes. The emission quenching induced by sequential addition of CT-DNA to 50 μM *rac*-**3** (λ_{ex} = 308 nm) is given in Fig. 6 (see Figs. S9 and S10 for

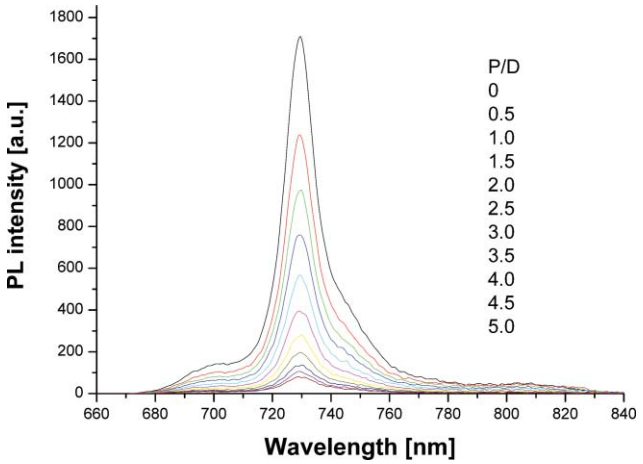

Fig. 6 Phosphorescence spectra of *rac*-[Cr(phen)$_2$(F$_2$dppz)](CF$_3$SO$_3$)$_3$ (*rac*-**3**) (50 μM in 100 mM phosphate buffer solution) in the presence of increasing concentration of CT-DNA (λ_{ex} = 308 nm).

rac-**1** and *rac*-**2** resp.†). The McGhee-von Hippel analysis of this quenching reveals binding parameters which are consistent with the absorption measurements (ESI Fig. S12†).

Given the charged nature of the complexes, the sensitivity of the binding to variations in the ionic strength was also investigated.[19] The steady-state emission of *rac*-**3** at a constant nucleotide:chromium (P/D) of 10 was examined upon addition of NaCl to the original buffered complex solution so as to eventually bring the salt concentration up to 300 mM NaCl. (Fig. 7). The results indicate that ionic strength has a significant influence on the DNA binding of the complex at concentrations greater than 30 mM NaCl. This was confirmed by also measuring the emission intensities over the P/D range 0-20 at various salt concentrations (*e.g.* at 50 mM NaCl {ESI Fig. S13†}). These studies point towards the importance of electrostatic interactions of the complex with DNA.

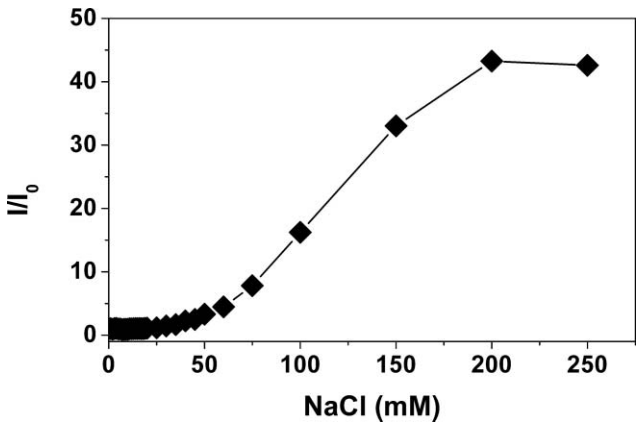

Fig. 7 The effect on the relative emission intensity (I/I_0) of the addition of NaCl to an aerated solution of *rac*-[Cr(phen)$_2$(F$_2$dppz)](CF$_3$SO$_3$)$_3$ (*rac*-**3**) in the presence of CT-DNA at P/D = 10. [Cr]= 15 μM in 10 mM phosphate buffer.

The magnitude of the emission intensity changes observed makes it an ideal method for probing the enantioselectivity of binding. Thus the effect of DNA binding on the emission of the Δ- and Λ- enantiomers of [Cr(phen)$_2$(dppz)](Cl)$_3$ (**1**) was also studied. The emission quenching behaviour of the enantiomers reveal similar binding strengths for each with CT-DNA in the 25 mM sodium phosphate buffer used (Fig. 8).

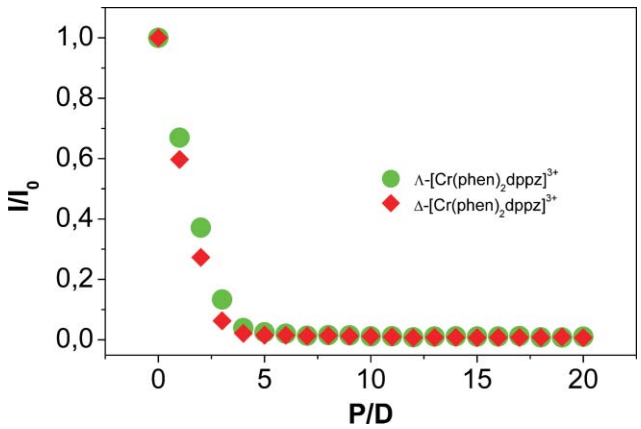

Fig. 8 Comparison of the intensity of phosphorescence (I) of Δ- and Λ-[Cr(phen)$_2$(dppz)](Cl)$_3$ in the presence of CT- DNA compared to that in its absence (I_0) (25 mM phosphate buffer solution, pH = 7; P/D = nucleotide:Cr; λ_{ex} = 370 nm).

2.3.3. Thermal denaturation. It is well known that compounds which intercalate between the basepairs of DNA can stabilise the duplex structure. This manifests itself as a characteristic change in the profile of the DNA melting curve (*i.e.* the temperature induced transition from double- to single-stranded DNA) obtained by monitoring the change in absorption at 260 nm with temperature. As shown in Fig. 9, addition of *rac*-**1** resulted in a significant broadening of the melting curve accompanied by an increase in melting temperature (T_m) compared to CT-DNA (indeed, denaturation is still incomplete at 90 °C). The observed behaviour is that expected for an intercalated compound and quite different from what would be observed if the compound was externally bound.[20]

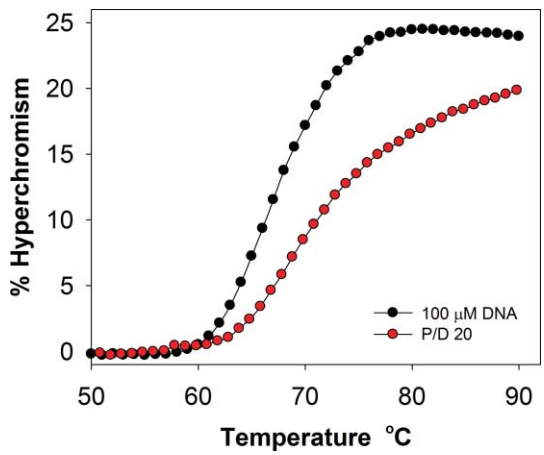

Fig. 9 Melting profile of CT-DNA (100 μM) in (a) the absence and (b) the presence of *rac*-**1** (5 μM) in 10 mM sodium phosphate buffer (pH = 7).

2.3.4 Linear dichroism studies. Linear dichroism (LD) spectroscopy may also be used to ascertain the mode by which complexes bind to flow-oriented CT-DNA. The spectra of

CT-DNA both free and in the presence of *rac*-**1-3** at P/D ratios of 10 : 1 can be seen in Fig. 10. The spectrum of the DNA itself exhibits a typical B-DNA profile with a negative LD signal at approximately 260 nm arising from the orientation of base pairs perpendicular to the DNA helical axis (and hence direction of flow). Upon the addition of the metal complexes this band was found to undergo a slight blueshift and increase in intensity, consistent with enhanced orientation or "stiffening" of the DNA helix. Such an effect is known to accompany the intercalation of small molecules into DNA. Furthermore, the introduction of the metal complexes induced additional negative LD bands at low P/D ratios, with one notably corresponding to the π–π^* absorption band of the X_2dppz ligand of the appropriate complex (*ca.* 370 nm, depending on the ligand). Such an observation is also consistent with intercalation, specifically the insertion of the dppz moiety into the DNA helix, parallel to the base pairs. Complex **2** induced somewhat larger negative LD signals than did equivalent ratios of complexes **1** and **3**, perhaps because of the greater intercalative ability of the more hydrophobic methyl-substituted dppz ligand.

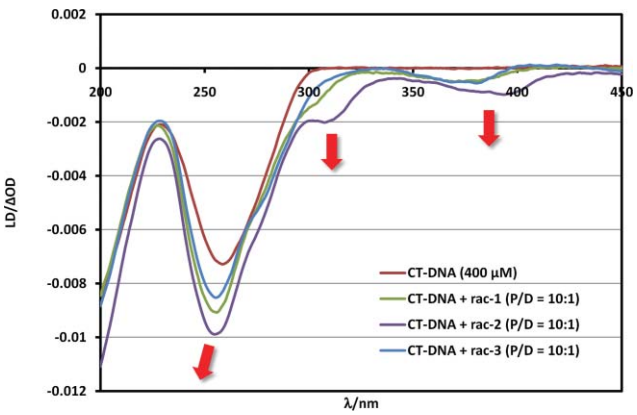

Fig. 10 LD spectra of free CT-DNA (400 μM) and CT-DNA in the presence of racemic complexes **1-3** at a P/D ratio of 10 : 1.

2.3.5. Circular Dichroism spectroscopy. Circular dichroism (CD) is a useful tool to measure the interaction of drugs with DNA.[21] The CD of unbound CT-DNA is characterised by a positive band at 275 nm and a negative band near 240 nm with a zero-crossover around 258 nm. These two bands are the net result of exciton coupling interactions of the bases which depend on the skewed orientation on the DNA backbone.[22] If the DNA is untwisted or the bases are tilted, any change in the base orientation should be reflected in the CD spectrum recorded below 300 nm. Any changes above 300 nm must solely originate from the bound compound under investigation.

Changes in CD were monitored upon addition of increasing quantities of *rac*-**1–3** to CT-DNA. In each case addition of the complex produced a negative band between 275 and 300 nm and a positive band at *ca.* 260 nm (Fig. 11 shows the effect of increased additions of *rac*-**2** to CT-DNA up to a $P/D = 5$; titrations with *rac*-**1** and *rac*-**3** yield similar results and are given in ESI Figs. S14 and S15†). The CD in the region 200 to 300 nm is expected to be complicated as it contains both changes induced in the DNA spectrum due to altered interactions of the bases and changes in the spectra of the enantiomers of the metal complex, as has already been reported for ruthenium complexes binding

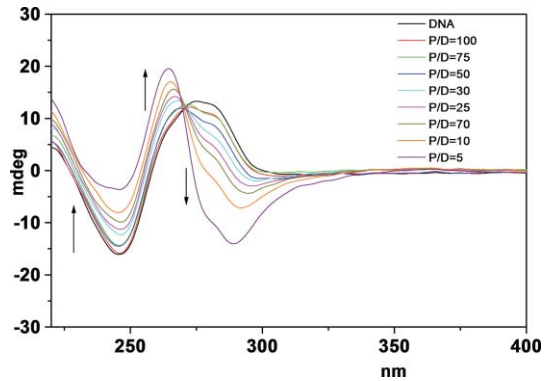

Fig. 11 CD spectra of titration of *rac*-$[Cr(phen)_2Me_2dppz](CF_3SO_3)_3$ (*rac*-**2**) with CT- DNA (150 μM) in 25 mM sodium phosphate buffer (pH = 7).

to DNA.[23,24] It is interesting that especially at the higher loading the CD spectrum has the features of the spectra of CT-DNA and the Δ-enantiomer. Similar behaviour has been reported for ruthenium complexes where this behaviour has been ascribed to an exciton-coupled induced circular dichroism ('ICD') arising due to *enantio*-preferential binding of the Δ enantiomer and/or ligand-ligand interactions of the bound/unbound complexes.[22-25]

The CD spectra of DNA-bound Δ- and Λ- enantiomers of $[Cr(phen)_2(dppz)](Cl)_3$ have also been examined (Fig. 12a and b). It may be observed that, in contrast to what is found for the *rac*-complexes in the presence of DNA these enantiomers exhibit a well-resolved band above 300 nm, which is already present at low loading and which grows steadily with successive additions of **1** to the DNA. At lower P/D the CD shows characteristics close to those of the free enantiomer, even though it is clear from the absorption and emission studies (*e.g.* Fig. 8) that the complexes are bound to the DNA under the experimental conditions of this CD experiment. Fig. 12c displays the spectra of the Δ- and Λ-enantiomers of **1** at a P/D = 10 and the sum of these spectra. This composite spectrum shows similar features overall to that observed experimentally for that of *rac*-**1** (ESI Fig S14†).

To probe the spectrum in the range 200-300 nm in more detail the 'Induced' CD spectra of DNA titration of Δ and Λ-$[Cr(phen)_2(dppz)](Cl)_3$ have been obtained, by subtracting the spectrum of DNA from the spectrum of the particular enantiomer in the presence of DNA (Fig. S17, S18†). It may be observed (Fig. 13) that these ICD spectra for the two enantiomers are strikingly different from each other indicating that while both are expected to be bound to the DNA, the effect of DNA-binding of the enantiomer on the CD spectrum is quite different. Whether this is due mainly to the effect of the DNA on the CD spectrum of the enantiomer of **1** or of the chromium complex on the DNA conformation cannot be determined at the moment, but it may be noted that the greatest change occurs in the region of π–π transitions for both the DNA bases and the dppz ligand.

3. Conclusions

We have prepared and resolved into their enantiomers a family of chromium complexes $[Cr(phen)_2(X_2dppz)]^{3+}$ {X = H, Me, or F} and compared their properties to those of the analogous properties of the widely-studied ruthenium complexes. Structurally, the

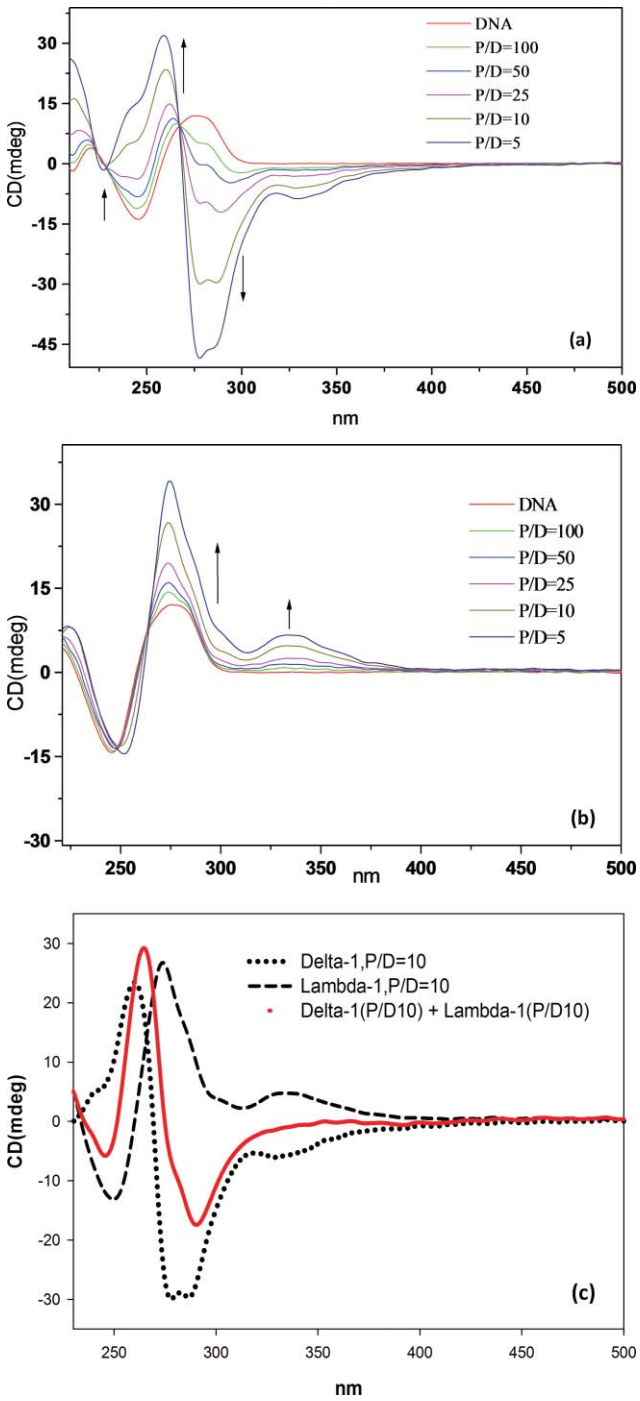

Fig. 12 CD spectra of titration of (a) Δ-$[Cr(phen)_2(dppz)](Cl)_3$ (b) Λ -$[Cr(phen)_2dppz](Cl)_3$ with CT-DNA (150 μM) in 25 mM sodium phosphate buffer (pH = 7). (c) Sum of CD spectra of Δ- and Λ -$[Cr(phen)_2dppz](Cl)_3$ at P/D = 10.

mean Cr–N distances at Cr(III) centre are 2.054 Å (*rac*-**1**) and 2.057 Å (*rac*-**3**), which are slightly shorter than those found for Ru–N in similar Ru(II) complexes $[Ru(dmp)_2(dppz)](PF_6)_3$ (2.104 Å)[26] and $[Ru(bpy)_2(dppz)(CN)_2](PF_6)_2$ (2.068 Å).[27] Similar to $[Ru(bpy)_2(dppz)(CN)_2](PF_6)_2$, the complexes dimerise in a centrosymmetric pair by π–π stacking between dppz ligands.[26]

A major difference, however, between the structurally analogous ruthenium(II) and chromium(III) complexes is that the lowest

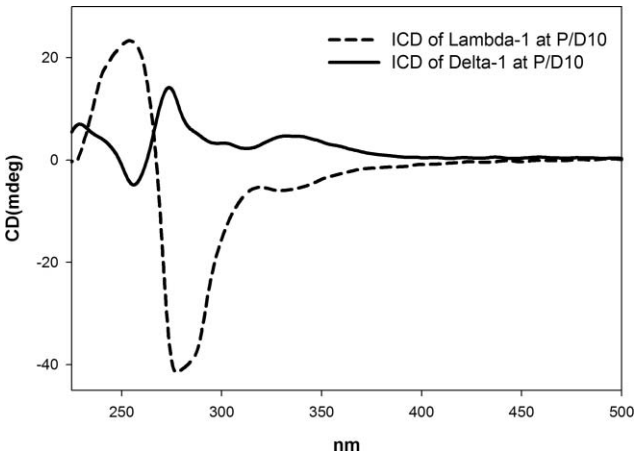

Fig. 13 ICD spectra of titration of Δ- and Λ-$[Cr(phen)_2(dppz)](Cl)_3$ with CT-DNA (150 μM) in 25 mM sodium phosphate buffer (pH = 7).

excited state of the $[Cr(phen)_2(X_2dppz)]^{3+}$ is metal-centred, in contrast to the MLCT state of the analogous ruthenium complex. The long-lived nature of this state and its narrow bandwidth make these compounds potentially interesting as nucleic acid probes. The energy of this state (1.70 eV) is unaffected by the substitution of the dppz ligand, although the excited state of the difluoro-species is a significantly stronger oxidising agent $\{E°[Cr(III)^*/Cr(II)] = 1.62$ V$\}$ than the unsubstituted and dimethyl species $\{E°[Cr(III)^*/Cr(II)] = 1.52$ and 1.49 V resp.$\}$, because of differences in their ground state redox properties. It may be noted that as a consequence of the low-lying metal-centred state $[Cr(phen)_2(F_2dppz)]^{3+}$ unlike $[Ru(phen)_2(F_2dppz)]^{3+}$ or $[Re(CO)_3(F_2dppz)py]^+$,[28] is strongly luminescent in aqueous solution

As already reported by Kane-Maguire and co-workers, *rac*-$[Cr(phen)_2(dppz)]^{3+}$ binds strongly to DNA.[9,10,16] In the current work we show by thermal denaturation and linear dichroism studies that fluorine or methyl substitution of the dppz ligand in its 11,12 position does not prevent intercalation between the base-pairs. Our current studies do not allow us to distinguish whether the complex enters from the major or the minor groove—a feature which has been debated for the analogous $[Ru(phen)_2(dppz)]^{2+}$.[29] Interestingly it is found that of the three complexes we have studied the dimethyl-derivative is the most strongly binding. A similar effect has been found for ruthenium complexes[17,18] and attributed to the hydrophobic effect of the alkyl group in the groove of the DNA. Very recently Kane-Maguire and coworkers have demonstrated that methyl substitution of the ancillary phenanthroline ligands in *rac*-$[Cr(Me_nphen)_2(dppz)]^{3+}$ (n = 2 or 4) does not greatly affect the strength of binding.[10c] The entropy of binding was positive in all cases and particularly large for $[Cr(Me_4phen)_2(dppz)]^{3+}$, which also showed strong enantioselective binding.

Our preliminary studies of $[Cr(phen)_2(X_2dppz)]^{3+}$ suggest that the binding affinity of each enantiomer is comparable, at least under the buffer conditions used (25 mM sodium phosphate). CD measurements do reveal a weakly negative signal characteristic of the Δ enantiomer at $\lambda > 300$ nm. This result would mirror the behaviour observed for the Δ-enantiomer of the ruthenium analogue $[Ru(phen)_2(dppz)]^{2+}$, which is known to show a slight preference for B-DNA.[3b,16] but further investigation is warranted

as this conclusion differs from that drawn by Kane-Maguire's group from dialysis studies,[16] where it was suggested that the Λ-enantiomer binds more strongly than its Δ-isomer.

The phosphorescence of each of the complexes is efficiently quenched upon binding to DNA. This is consistent with the strong oxidising power of the complexes' excited state, which is greater than that required to oxidise guanine.[30] It may be noted that the efficiency of quenching upon binding to this natural mixed sequence DNA is much higher than that observed for $[Ru(TAP)_2(dppz)]^{2+}$.[4a] Whether this is due to specificity of binding to a particular site on the DNA or to a different (more rapid) mechanism of quenching (direct electron transfer *versus* proton-coupled electron transfer) remains to be elucidated. The photophysics of the $[Cr(phen)_2(X_2dppz)]^{3+}$ {X = H, Me, or F} in the presence of nucleic acids will be the subject of a forthcoming publication. The properties and binding phenomena described here add further support to the potential of intercalating chromium complexes as nucleic acid probes.

4. Experimental

Materials and methods

All chemicals and solvents were commercially purchased and used as received. 1,10-phenanthroline (≥99%), trifluoromethanesulfonic acid (98%), potassium hexafluorophosphate (KPF_6, 98%), (-)-*O*,*O*′-dibenzoyl-L-tartaric acid monohydrate (≥99%), Sephadex C-25, Dowex 1 × 8-200 and Calf Thymus B-DNA (CT-DNA) were purchased from Sigma Aldrich. CT-DNA concentrations were determined spectrophotometrically using the molar extinction coefficient of ε_{260} = 6600 M^{-1} cm^{-1}. Amberlite IRA-402 and tetrabutylammonium chloride (≥99%) were obtained from Fluka; $CrCl_3.6H_2O$ was obtained from BDH.

Absorption spectra were obtained on a Varian Cary 50 or a Shimadzu 2401 UV/vis spectrometer. Steady-state emission data were collected on a Perkin Elmer L55 (used in the phosphorescence mode) in air saturated solutions at room temperature. Mass spectra were recorded on an LCT Orthogonal Acceleration TOF Electrospray Mass spectrometer. Electrochemical measurements were made on a CHI660C workstation using a Ag/AgCl reference electrode (potential of 0.20 V *vs.* NHE). Circular dichroism studies were performed on a Jasco J-810 spectropolarimeter and flow-oriented linear dichroism studies were performed on a Jasco J-815 CD spectrometer fitted with a Dioptica Scientific Ltd. Linear Dichroism 2 apparatus. The DNA and Cr complex solutions for all titrations were prepared in (25 mM or 100 mM) sodium phosphate buffer (pH=7). UV/vis absorption data on DNA titrations were collected by increased volumetric addition of CT-DNA to 2.5 ml of a Cr complex solution in a 1 cm quartz cuvette up to a [Nucleic Acid]: [Cr complex] ratio (P/D) of 20. CD titrations were carried out in 25 mM sodium phosphate buffer (pH = 7) medium, by addition of aliquots of 55 μM Cr(III) complex solutions to CT-DNA (150 μM). Thermal denaturation experiments were performed on a Cary 300 Spectrometer equipped with a multicell Peltier stage. The temperature in the cell was ramped from 20 to 90 °C, at a rate of 1 °C min^{-1} and the absorbance at 260 nm of CT-DNA (150 μM) at 260 nm in 10 mM phosphate buffer at pH 7 in the absence and presence of the metal complex at a P/D of 20 was measured every 0.2 °C.

Synthesis of ligands and complexes

The ligands dppz (dipyrido-[3,2-a:2′-,3′-c]-phenazine) and its substituted derivatives Me_2dppz and F_2dppz were synthesised by the condensation of 1,10-phenathroline-5,6-dione[11] with the appropriate diamino compounds.[12] They were further purified on Al_2O_3 columns using a solvent system 5-95 MeOH–CH_2Cl_2.

$[Cr(phen)_2Cl_2]Cl{\cdot}2H_2O$ was prepared from 1,10-phenanthroline and $CrCl_3{\cdot}6H_2O$ using the literature method for the analogous bis-bipyridine complex[31] and recrystallised to remove traces of catalytic zinc.

Preparation of $[Cr(phen)_2(CF_3SO_3)_2](CF_3SO_3)$

$[Cr(phen)_2(CF_3SO_3)_2](CF_3SO_3)$ was prepared by a modification of the literature method.[3b,13] Trifluoromethanesulfonic acid (10 g) was added to $[Cr(phen)_2Cl_2]Cl{\cdot}2H_2O$ (*ca.* 1 g, 1.80 × 10^{-3} mol) under an atmosphere of nitrogen. The resultant reddish brown solution was heated to 100 °C and a stream of nitrogen bubbled through it until the evolution of HCl had ceased (approximately 4 h, at which point the effluent gas no longer produced an AgCl precipitate when bubbled through an aqueous solution of $AgNO_3$). While maintaining the atmosphere of nitrogen the solution was cooled on ice and, with vigorous stirring, anhydrous diethylether was added dropwise *via* a syringe and septum until formation of a pink precipitate was complete (*ca.* 30 mL). The product was purified by repeated centrifugation in fresh anhydrous diethylether. Due to the apparent air sensitivity of the complex, the complex was stored in the dessicator under vacuum until required for the next step in the synthesis. Yield: *ca.* 500 mg (32%). The success of this synthesis was found to be quite sensitive to the sample of trifluoromethanesulfonic acid used.

Preparation of *rac*-$[Cr(phen)_2(dppz)](CF_3SO_3)_3$ (1)

$[Cr(phen)_2(dppz)](CF_3SO_3)_3$ was prepared by reported methods[13] before being further purified using cation exchange chromatography on CM Sephadex C-25 with an aqueous 0.5 M NaCl solution as the eluent. The PF_6^- salt was isolated from the eluate by the addition of KPF_6 and subsequent filtration to collect the yellow precipitate. **UV/vis** (MeCN): ε(356 nm) = 16,100 M^{-1} cm^{-1}, ε(374 nm) = 12,900 M^{-1} cm^{-1}.

Preparation of *rac*-$[Cr(phen)_2(Me_2dppz)](CF_3SO_3)_3$ (2)

$[Cr(phen)_2(CF_3SO_3)_2](CF_3SO_3)$ (105 mg, 1.02 × 10^{-4} mol) was refluxed with Me_2dppz (47.8 mg, 1.54 × 10^{-4} mol) in dichloromethane (45 ml) for 18 h. The yellow solid produced was filtered under vacuuo, washed with dichloromethane (40 ml) and then with diethylether (50 ml) and kept in a vacuum desiccator over P_2O_5. The PF_6^- salt of the complex was obtained as per (**1**). **Yield**: 62.3 mg (41%), **UV/vis** (MeCN): ε(367 nm) = 19,300 M^{-1} cm^{-1}, ε(386 nm) = 19,950 M^{-1} cm^{-1}. **ES-MS** (MeCN): Calc. mass *m*/*z* 722.1999, Actual mass *m*/*z* 722.2017, $[Cr(phen)_2(Me_2dppz)]^{3+}$, $C_{44}H_{30}N_8Cr$.

Preparation of *rac*-$[Cr(phen)_2(F_2dppz)](CF_3SO_3)_3$ (3)

$[Cr(phen)_2(F_2dppz)](CF_3SO_3)_3$ was synthesised by a similar procedure as above, except that F_2dppz (49 mg, 1.54 × 10^{-4} mol) was used instead of Me_2dppz. The PF_6^- salt of the complex

was obtained as per (**1**). **Yield**: 72.7 mg (47%), **UV/vis** (MeCN): ε(356 nm) = 18,690 M^{-1} cm^{-1}, ε(374 nm) = 19,350 M^{-1} cm^{-1}. **ES-MS** (H_2O): Calc. mass *m*/*z* 730.1497, Actual mass *m*/*z* 730.1514, $[Cr(phen)_2(F_2dppz)]^{3+}$, $C_{42}H_{24}N_8F_2Cr$.

Separation of enantiomers of $[Cr(phen)_2X_2(dppz)](CF_3SO_3)_3$

The two enantiomers were sucessfully resolved chromatographically on Sephadex C-25. The resolution was carried out by introducing an aq. solution of *rac*-$[Cr(phen)_2(X_2dppz)](CF_3SO_3)_3$ (*ca*. 40 mg) on a C-25 column with 0.1 M sodium (-)-*O*,*O*′-dibenzoyl-L-tartrate as the eluent at 2 ml min^{-1} flow rate recycled by a peristaltic pump.[32] Within a single pass down a column 1 m in length the two enantiomers were separated as distinct yellow bands. The fractions were collected separately, precipitated as PF_6^- salts by adding KPF_6, and subsequently isolated by suction filtration or extraction into and subsequent evaporation of CH_2Cl_2 (this latter technique resulted in lower yields due to the limited solubility of the complexes in CH_2Cl_2). The two fractions were characterised using circular dichroism spectroscopy; by comparison with previously reported spectra[15,16] the first eluted band of each complex was identified as the Λ enantiomer, the second band as the Δ enantiomer.

Studies into the DNA interactions of the resolved enantiomers required the conversion of the PF_6^- salts of the complexes into water-soluble Cl^- salts. This was accomplished by dissolving the PF_6^- salts in a minimum volume of acetone and stirring this solution with a methanolic slurry of an appropriate anion-exchange resin (Amberlite IRA-402 or Dowex 1 × 8-200) until a uniformly transparent solution was obtained. The solution was subsequently filtered and evaporated to dryness on a rotary evaporator to obtain the chloride salt of the desired enantiomer.

Λ-$[Cr(phen)_2(dppz)]^{3+}$- **UV/vis (H_2O):** 378, 358 nm. **ES-MS (MeCN):** Calc. mass *m*/*z* 694.1686, Actual mass *m*/*z* 694.1673, $[Cr(phen)_2(dppz)]^{3+}$, $C_{42}H_{26}N_8Cr$.

Δ-$[Cr(phen)_2(dppz)]^{3+}$–**UV/vis (H_2O):** 378, 358 nm. **ES-MS (MeCN):** Calc. mass *m*/*z* 694.1686, Actual mass *m*/*z* 694.1661, $[Cr(phen)_2(dppz)]^{3+}$, $C_{42}H_{26}N_8Cr$.

X-ray crystallography

The data for crystals 1 and 2 were collected on a Rigaku Saturn 724 CCD Diffractometer. Suitable crystals from each compound were selected and mounted using an inert oil on a 0.30 mm quartz fibre tip and immediately placed on the goniometer head in a 153 K N2 gas stream. The data sets were collected using Crystalclear-SM 1.4.0 software and 1680 diffraction images, of 0.5° per image, were recorded. Data integrations, reductions and corrections for absorption and polarization effects were all performed using Crystalclear-SM 1.4.0 software. Space group determinations, structure solutions and refinements were obtained using Crystalstructure ver. 3.8 and Shelxtl* ver. 6.14 software.§

Crystal data and structural refinement parameters:

$[Cr(phen)_2(dppz)](CF_3SO_3)_3$: E.F. $C_{45}H_{26}CrF_9N_8O_9S_3$, F.W.= 1141.92, Triclinic, Space group $P\bar{1}$; a = 10.331(3), b = 13.214(3), c = 19.073(5) Å, α = 72.494(18), β = 74.473(19), γ = 68.319(15)°; U = 2271.0(10) Å^3; Z = 2; D_c = 1.670 Mg m^{-3}; μ = 0.495 mm^{-1}; θ Range for data collection = 2.84–25.00; Reflections collected 35508, Unique Reflections 6722 [R_{int}=0.0726]; Data/restraints/parameters 7991/0/677; Goodness-of-fit on F^2 1.211; R indices (all data) = R_1 = 0.1069, wR_2 = 0.1531; Final R indices [$I > 2\sigma(I)$] = R_1 = 0.0873, wR_2 = 0.1451.

$[Cr(phen)_2(F_2dppz)](CF_3SO_3)_3$: E.F. $C_{45}H_{26}CrF_9N_8O_9S_3$, F.W.= 1141.92, Triclinic, Space group $P\bar{1}$; a = 10.2634(14), b = 13.262(2), c = 19.284(3) Å, α = 73.745(7), β = 74.983(8), γ = 67.915(8)°; U = 2299.8(6) Å^3; Z = 2; D_c = 1.701 Mg m^{-3}; μ = 0.498 mm^{-1}; θ Range for data collection = 1.12–25.00; Reflections collected 18396, Unique Reflections 6379 [R_{int}=0.0339]; Data/restraints/parameters 7288/0/695; Goodness-of-fit on F^2 1.024; R indices (all data) = R_1 = 0.0549, wR_2 = 0.1769; Final R indices [$I > 2\sigma(I)$] = R_1 = 0.0475, wR_2 = 0.1508.

§ Software Reference Manual, version 5.625, Bruker Analytical X-Ray Systems Inc., Madison, WI, 2001. Sheldrick, G. M. SHELXTL, An Integrated System for Data Collection, Processing, Structure Solution and Refinement, Bruker Analytical X-Ray Systems Inc., Madison, WI, 2001.

Acknowledgements

SV and JAS thank IRCSET for the award of postdoctoral fellowships. The HEA (PRLTI4/CSCB) and SFI (06/CHP036 and 07/CHEF437) are thanked for their financial support. We are grateful to Dr Martin Feeney for recording the mass spectra.

Notes and references

1 (*a*) J. Cadet, T. Douki, D. Gasparutto and J.-L. Ravanat, *Mutat. Res., Fundam. Mol. Mech. Mutagen.*, 2003, **531**, 5; (*b*) C. G. Barry, E. C. Turney, C. S. Day, G. Saluta, G. L. Kucera and U. Bierbach, *Inorg. Chem.*, 2002, **41**, 7159; (*c*) K. Karidi, A. Garoufis, N. Hadjiliadis, M. Lutz, A. L. Spek and J. Reedijk, *Inorg. Chem.*, 2006, **45**, 10282; (*d*) S. W. Magennis, A. Habtemariam, O. Novakova, J. B. Henry, S. Meier, S. Parsons, I. D. H. Oswald, V. Brabec and P. J. Sadler, *Inorg. Chem.*, 2007, **46**, 5059.

2 (*a*) J. G. Vos and J. M. Kelly, *Dalton Trans.*, 2006, 4869; (*b*) B. M. Zeglis, V. C. Pierre and J. K. Barton, *Chem. Commun.*, 2007, 4565; (*c*) B. Elias and A. Kirsch–De Mesmaeker, *Coord. Chem. Rev.*, 2006, **250**, 1627; (*d*) C. Moucheron, *New J. Chem.*, 2009, **33**, 235.

3 (*a*) A. E. Friedman, J.-C. Chambron, J.-P. Sauvage, N. J. Turro and J. K. Barton, *J. Am. Chem. Soc.*, 1990, **112**, 4960; (*b*) I. Haq, P. Lincoln, D. Suh, B. Nordén, B. Z. Chowdhry and J. B. Chaires, *J. Am. Chem. Soc.*, 1995, **117**, 4788; (*c*) E. J. C. Olson, D. Hu, A. Hörmann, A. M. Jonkman, M. R. Arkin, E. D. A. Stemp, J. K. Barton and P. F. Barbara, *J. Am. Chem. Soc.*, 1997, **119**, 11458; (*d*) M. K. Brennaman, J. H. Alstrum-Acevedo, C. N. Flemming, P. Jang, T. J. Meyer and J. M. Papanikolas, *J. Am. Chem. Soc.*, 2002, **124**, 15094; (*e*) B. Önfelt, J. Olofsson, P. Lincoln and B. Nordén, *J. Phys. Chem. A*, 2003, **107**, 1000.

4 (*a*) I. Ortmans, B. Elias, J. M. Kelly, C. Moucheron and A. Kirsch-De Mesmaeker, *Dalton Trans.*, 2004, 668; (*b*) B. Elias, C. Creely, G. W. Doorley, M. M. Feeney, C. Moucheron, A. Kirsch-De Mesmaeker, J. Dyer, D. C. Grills, M. W. George, P. Matousek, A. W. Parker, M. Towrie and J. M. Kelly, *Chem.–Eur. J.*, 2008, **14**, 369.

5 W. Lu, D. A. Vicic and J. K. Barton, *Inorg. Chem.*, 2005, **44**, 7970.

6 F. Shao and J. K. Barton, *J. Am. Chem. Soc.*, 2007, **129**, 14733.

7 A. M. Angeles-Boza, P. M. Bradely, P. K.-L. Fu, S. E. Wicke, J. Bacsca, K. R. Dunbar and C. Turro, *Inorg. Chem.*, 2004, **43**, 8510.

8 (*a*) H. D. Stoeffler, N. B. Thornton, S. L. Temkin and K. S. Schanze, *J. Am. Chem. Soc.*, 1995, **117**, 7119; (*b*) V. W.-W. Yam, K. K.-W. Lo, K.-K. Cheung and R. Y.-C. Kong, *J. Chem. Soc., Dalton Trans.*, 1997, 2067.

9 (*a*) K. D. Barker, K. A. Barnett, S. M. Connell, J. W. Glaeser, A. J. Wallace, J. Wildsmith, B. J. Herbert, J. F. Wheeler and N. A. P. Kane-Maguire, *Inorg. Chim. Acta*, 2001, **316**, 41; (*b*) E. G. Donnay, J. P. Schaeper, R. D. Brooksbank, J. L. Fox, R. G. Potts, R. M. Davidson, J. F. Wheeler and N. A. P. Kane-Maguire, *Inorg. Chim. Acta*, 2007, **360**, 3272.

10 (*a*) N. A. P. Kane-Maguire and J. F. Wheeler, *Coord. Chem. Rev.*, 2001, **211**, 145; (*b*) N. A. P. Kane-Maguire, *Top. Curr. Chem.*, 2007, **280**,

37; (*c*) M. S. Vandiver, E. P. Bridges, R. L. Koon, A. N. Kinnaird, J. W. Glaeser, J. F. Campbell, C. J. Priedemann, W. T. Rosenblatt, B. J. Herbert, S. K. Wheeler, J. F. Wheeler and N. A. P. Kane-Maguire, *Inorg. Chem.*, 2010, **49**, 839–848.
11 R. D. Gillard, R. E. E. Hill and R. Maskill, *J. Chem. Soc. A*, 1970, 1447.
12 J. E. Dickeson and L. A. Summers, *Aust. J. Chem.*, 1970, **23**, 1023.
13 C. K. Ryu and J. F. Endicott, *Inorg. Chem.*, 1988, **27**, 2203.
14 M. Isaacs, A. G. Sykes and S. Ronco, *Inorg. Chim. Acta*, 2006, **359**, 3847.
15 M. Ardhammar, P. Lincoln, A. Rodger and B. Nordén, *Chem. Phys. Lett.*, 2002, **354**, 44.
16 K. D. Barker, B. R. Benoit, J. A. Bordelon, R. J. Davis, A. S. Delmas, O. V. Mytykh, J. T. Petty, J. F. Wheeler and N. A. P. Kane-Maguire, *Inorg. Chim. Acta*, 2001, **322**, 74.
17 J. Olofsson, L. M. Wilhelmsson and P. Lincoln, *J. Am. Chem. Soc.*, 2004, **126**, 15458.
18 K. O'Donoghue, J. C. Penedo, J. M. Kelly and P. E. Kruger, *Dalton Trans.*, 2005, 1123.
19 (*a*) F. M. O'Reilly and J. M. Kelly, *New J. Chem.*, 1998, **22**, 215; (*b*) F. M. O'Reilly and J. M. Kelly, *J. Phys. Chem. B*, 2000, **104**, 7206.
20 J. M. Kelly, A. B. Tossi, D. J. McConnell and C. OhUigin, *Nucleic Acids Res.*, 1985, **13**, 6017.
21 N. Berova, K. Nakanishi and R. W. Woody, (ed.), (*Circular Dichroism: Principles and applications*, Second Ed., 2000, John Wiley and Son, Inc.
22 A. Rodger and B. Nordén, *Circular Dichroism and Linear Dichroism*, 1997, Oxford Chemistry Press, UK.
23 C. Hiort, P. Lincoln and B. Nordén, *J. Am. Chem. Soc.*, 1993, **115**, 3448.
24 S.-D. Choi, M.-S. Kim, S. K. Kim, P. Lincoln, E. Tuite and B. Nordén, *Biochemistry*, 1997, **36**, 214.
25 P. U. Maheswari, V. Rajendiran, H. Stoeckli-Evans and M. Palaniandavar, *Inorg. Chem.*, 2006, **45**, 37.
26 J.-G. Liu, Q.-L. Zhang, X.-F. Shi and L.-N. Ji, *Inorg. Chem.*, 2001, **40**, 5045.
27 J. Rusanova, S. Decurtins, E. Rusanov, H. Stoeckli-Evans, S. Delahaye and A. Hauser, *J. Chem. Soc., Dalton Trans.*, 2002, 4318.
28 J. Dyer, C. M. Creely, J. C. Penedo, D. C. Grills, S. Hudson, P. Matousek, A. W. Parker, M. Towrie, J. M. Kelly and M. W. George, *Photochem. Photobiol. Sci.*, 2007, **6**, 741–748.
29 (*a*) E. Tuite, P. Lincoln and B. Norden, *J. Am. Chem. Soc.*, 1997, **119**, 239; (*b*) R. E. Holmlin, E. D. Stemp and J. K. Barton, *Inorg. Chem.*, 1998, **37**, 29; (*c*) A. Greguric, I. D. Greguric, T. W. Hambley, J. Aldrich-Wright and J. G. Collins, *J. Chem. Soc., Dalton Trans.*, 2002, 849.
30 S. S. Shinde, A. Maroz, M. P. Hay and R. F. Anderson, *J. Am. Chem. Soc.*, 2009, **131**, 5203.
31 F. H. Burstall and R. S. Nyholm, *J. Chem. Soc.*, 1952, 3570.
32 N. C. Fletcher, P. C. Junk, D. A. Reitsma and F. R. Keene, *J. Chem. Soc., Dalton Trans.*, 1998, 133.

